2020 IEEE/RSJ International Conference on Intelligent Robots and Systems (IROS)
October 25-29, 2020, Las Vegas, NV, USA (Virtual)

Intermittent Insertion Control Method with Fine Needle for Adapting Lung Deformation due to Breathing Motion

Ryosuke Tsumura, *Member, IEEE*, Kaoru Kakima and Hiroyasu Iwata, *Member, IEEE*

***Abstract*—Fine needle insertions into a lung are challenging in terms of the needle deflection due to the breathing motion. Although previous related works neglected the effect for the needle deflection due to the breathing motion by patients stopping the breath during the insertion, they have to suffer from the discomfort. This paper proposes the intermittent insertion control method to decrease needle deflection adapting the lung deformation due to the breathing motion. The novelty of this method is to allow for accurate needle insertion without stopping the breath, which will contribute to decreasing the discomfort and the amount of radiation exposure for patients. The intermittent insertion is to move forward the fine needle during a certain time frame that the needle deflection barely occurs since the lung is not deformed by the diaphragm motion. The feasibility of the proposed method was validated through a polyvinyl chloride (PVC) phantom and ex vivo experiments. The results showed that the deflection can be suppressed up to 1.3 mm and 3.9 mm in the PVC phantom and ex vivo experiments, respectively.**

I. Introduction

Percutaneous needle insertion has been a common surgical option of cancer diagnosis and treatment instead of open surgery, such as biopsy, radiofrequency ablation (RFA), and brachytherapy. These procedures are commonly performed manually by physicians under medical imaging modalities, such as computed tomography (CT), magnetic resonance imaging (MRI), and ultrasound (US) imaging, to provide feedback information to guide the needle to the target. Lung cancer is the leading cause of cancer deaths worldwide and the main target that the diagnosis and treatment with percutaneous needle insertion are applicable. For the early detection of cancer, the biopsy is usually performed once observing a suspicious legion with CT images [1]. The RFA which is the technique to heat tumors locally through the needle under the CT guidance is also the main option of lung cancer treatment [2]. In both procedures, the CT scan is basically performed to observe the position of tumors and establish the path plan of needle insertion preoperatively [3]. During the needle insertion into the lung, the physicians conform the needle insertion path is the correct direction into targets avoiding anatomical obstacles. Once inserting the needle to an unintended direction, the physicians have to retract the needle and need to scan additional CT images. Repeating the procedures causes increasing not only the amount of radiation exposure [4] but also the risk of complications such as hematoma [5]–[7]. Additionally, the physicians need to go back and forward to the CT room each time to take the new CT scan, and subsequently the whole procedure is delay [3].

*Research supported by Hasumi International Research Institution.
R. Tsumura is with the Global Robot Academia Laboratory, Waseda University, Tokyo, Japan (e-mail: ryosuke-tsumura@iwata.mech.waseda.ac.jp).
K. Kakima is with the School of Creative Science and Engineering, Waseda University, Tokyo, Japan.
H. Iwata is with the Faculty of Science and Engineering, Waseda University, Tokyo, Japan

The accuracy of the needle insertion is generally caused due to the needle deflection and tissue deformation in addition to the lack of target visibility [8]. The degree of needle deflection is significantly depending on the needle gauge. A fine needle with a bevel-tip is naturally deflected following a circular trajectory [9]–[12]. Moreover, in the case of the lung needle insertion, a drastic tissue deformation due to breathing motions occurs [13], which may cause the deflection additionally. Meanwhile, fine needle insertion allows for low tissue damages and reducing the risk of complications (e.g. hematoma, seeding, and pneumothorax) [7], [14]–[18]. Especially, the amount of bleeding is related to the needle size [19]. Therefore, there is a demand for the technology to perform accurate needle insertion with minimum CT scans in the lung.

A. Related Works

Numerous robotic needle insertion systems aiming to the accurate placement under medical imaging modalities have been proposed in those days. As one of the mainstreams in this field, a needle steering which controls the trajectory with the needle deflection generated by using flexible fine needles with the bevel-tip is widely developed [20]–[22]. During the needle insertion into a soft-tissue, the interaction force between the needle and the surrounding tissue (e.g. cutting force) is applied to the bevel-tip and causes the transverse load [23], [24]. By modeling the needle deflection (e.g. kinematic and mechanics-based model [25]), the trajectory can be pre-defined. To compensate for the error of the deflection model and satisfy the safety for patients, closed-loop control is applied with real-time feedback from the needle tip position. In order to track the needle tip real-time, US [25]–[29], MRI [30], [31], and CT [32], [33] were used as the guidance. In the lung needle insertion, the CT scan is generally used as mentioned above. Then, it is not desirable to track the needle in real-time with the CT scan in terms of radiation exposure. Also, during the needle insertion into the lung, since the tissue deformation occurs due to the breathing motion, it is questionable to apply the proposed deflection model and needle steering.

There are several researches focusing on the robotic needle insertion system targeting the lung. The previous researches can be divided into two categories. First, the robot systems [33]–[35] are proposed as a given that patients can stop the breathing during the needle insertion and then the effect of the

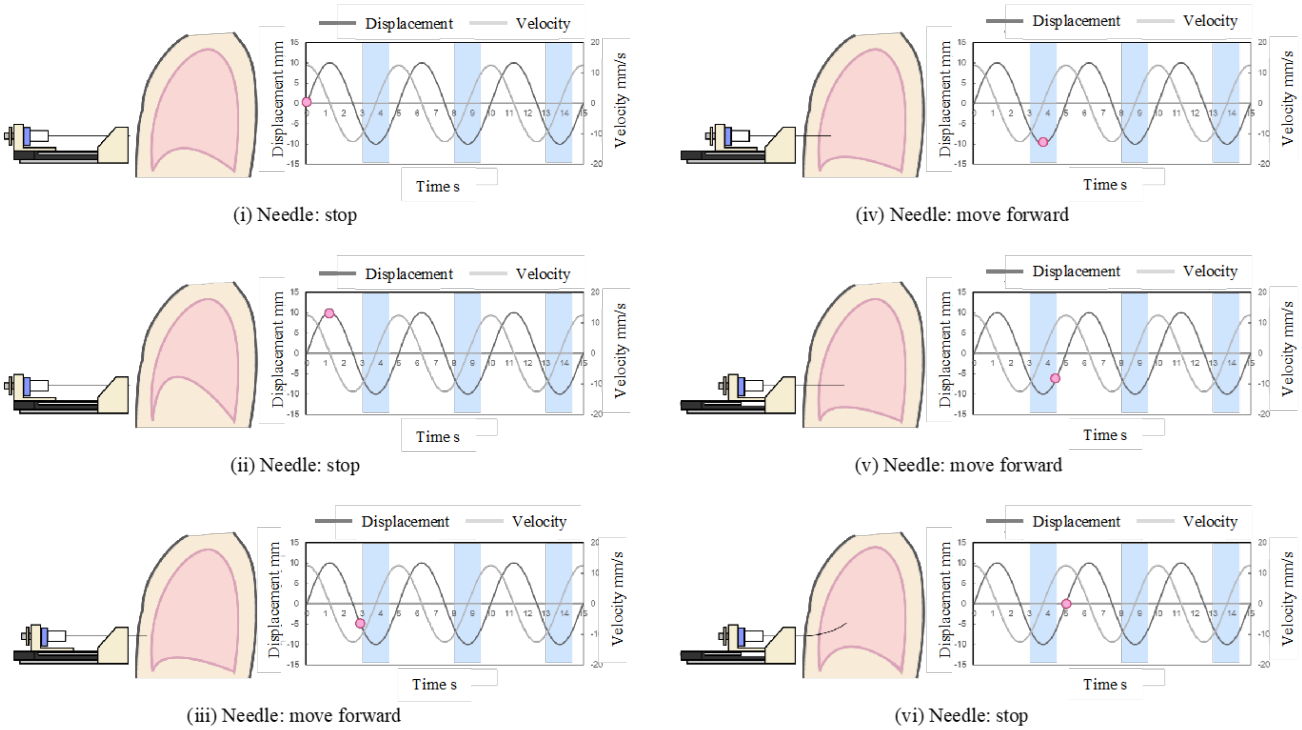

Fig. 1 Sequential overview of the intermittent needle insertion: left illustration shows the relationship between the needle and diaphragm motion and right graph shows the displacement (black line) and velocity (gray line) of the diaphragm during breath cycle (red dot: current time corresponding the left picture, blue area: time frame to move forward the needle) in each image.

breathing for the needle deflection is negligible. Under the condition, the needle steering may be applicable in the lung. Meanwhile, the patients suffer from a discomfort caused by stopping the breathing. Also, certain percentages of patients cannot be covered due to the difficulty of stopping the breathing. Second, it is proposed that the robot systems can perform a very fast needle insertion (100-600 mm/s) finding an optimal time [36], [37]. This approach can also neglect the effect of the breathing motion since the time to insert the needle into the target is very short. Those robot systems also used a thick needle which barely causes the needle deflection. Meanwhile, the risk of pneumothorax is increased by using the thick needle and more importantly, such the fast insertion with the thick needle may not be acceptable in term of the safety for patients.

B. Contribution

This paper presents a new insertion control method with the fine needle which allows for reducing the needle deflection due to the breathing motion. The limitation of the related works is to premise that the effect of breathing motion for the needle insertion is negligible. However, the internal tissue motion due to the breathing motion must occur in real situations and may cause to decrease the accuracy of the needle insertion, especially with the fine needle. Ultimately, it is desirable to reach the fine needle into the target without holding breath because of reducing the risk of complications and the discomfort for patients. Our hypothesis is that by moving forward the needle intermittently at certain time frame during breathing cycle, the needle deflection due to the breathing motion can be suppressed without holding breath. We investigate the effect for the needle deflection due to the breathing motion experimentally to support our hypothesis at first. Then, the proposed method is demonstrated via phantom and *ex vivo* experiments. To the best of our knowledge, we believe to propose a first robotic lung insertion method with the fine needle to reduce the deflection due to breathing motion.

II. Method

A. Intermittent Insertion Method

Lung adenocarcinoma is the most common type of lung cancer and often occurs at lower lung filed where the tissue is significantly deformed due to a diaphragm motion. The range of the diaphragm motion is about 8-30 mm [13]. Then, we assume the diaphragm motion leads to the internal tissue deformation, which may cause further needle deflections. There are several approaches to decrease the needle deflection by applying the rotation [38]–[40]. We also previously proposed the insertion method to minimize the needle deflection and tissue damages by combing bidirectional rotation and vibration with an extra-fine needle (25 gauge; φ0.5 mm) [41], [42]. Meanwhile, we assume that once the internal tissue motion occurs during the needle insertion, the needle deviates from the intended trajectory even applying the rotation to the needle.

To address the internal tissue motion, we propose the intermittent needle insertion method which repeats to move forward the needle at a certain time frame during the breathing cycle when the needle deflection doesn't occur and to stop the needle at the other time frame as shown in Fig. 1. The proposed insertion method allows patients for the breath during the needle insertion and perform the procedure with low tissue damage because of the fine flexible needle. Fig. 2 shows that the conceptual insertion control diagram. The time frame

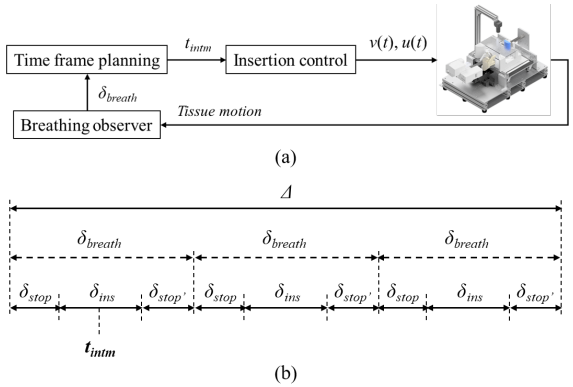

Fig. 2 Conceptual control design: (a) the control diagram includes the time frame planning for the intermittent insertion, insertion control and breathing observer, (b) the procedure time duration (Δ) is split into multiple (e.g. three) cycles of breathing duration (δ_{breath}). In each breath cycle, the needle is moved forward at the timing (t_{intm}) for certain time frame (δ_{ins}) and stops in other time durations (δ_{stop}).

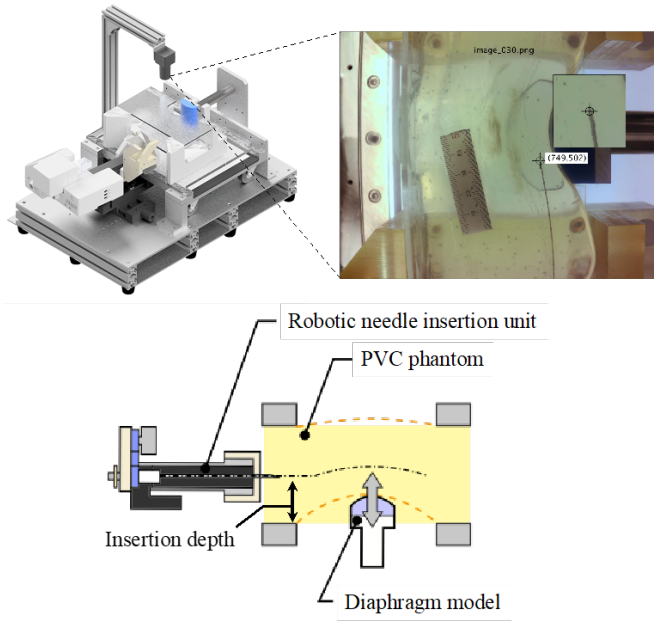

Fig. 3 Experimental setup is composed of robotic needle insertion unit, diaphragm model, PVC phantom, and camera to measure the needle tip position. The diaphragm motion is synchronized with the needle insertion motion.

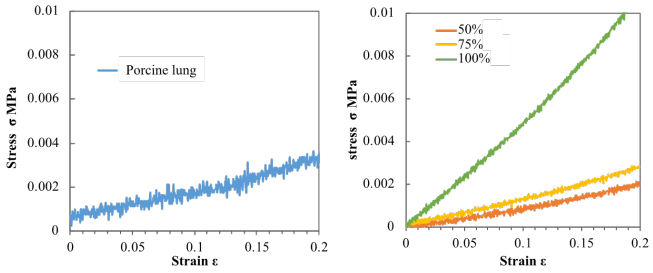

Fig. 4 Comparison of tissue stiffness between porcine lung (left graph) and PVC phantoms with different softener ratios (right graph).

planning output the time to conduct the intermittent insertion t_{intm} based on the breathing duration time δ_{breath} generated by the breathing observer. The robotic needle insertion system

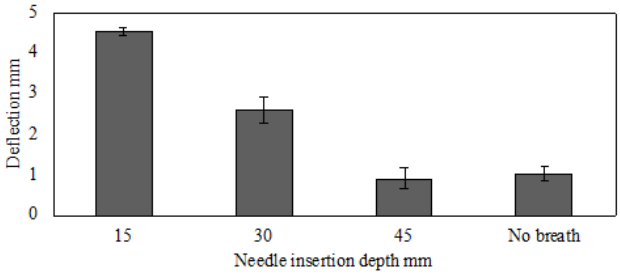

Fig. 5 The comparison of the deflection in several insertion depths under breaching motion and without breathing motion as a grand truth.

performs the needle insertion and rotation motions corresponding to the t_{intm} as following:

$$v(t) = \begin{cases} v_{ins}, & t_{intm} - \delta_{ins}/2 \le t \le t_{intm} + \delta_{ins}/2 \\ 0, & t < t_{intm} - \delta_{ins}/2, t_{intm} + \delta_{ins}/2 < t \end{cases}$$
$$u(t) = \begin{cases} u_{rot}, & t_{intm} - \delta_{ins}/2 \le t \le t_{intm} + \delta_{ins}/2 \\ 0, & t < t_{intm} - \delta_{ins}/2, t_{intm} + \delta_{ins}/2 < t \end{cases} \quad (1)$$

v and u represent the insertion and rotation velocities, respectively. t shows the procedure time during one cycle of breathing motion. δ_{ins} represents the duration time to move forward the needle. In following sections, we describe the effect for the needle deflection due to the breathing motion and the determination of the optimal time frame to move forward the needle intermittently through preliminary experiments.

B. Analysis of Breathing Motion

The quantitative effect for the needle deflection due to the breathing motion is still questionable. Especially, we assume that the degree of the needle deflection is depending on the distance between the trajectory path and the diaphragm. Then, we investigate the needle deflection due to the breathing motion through a phantom study as a preliminary experiment. Experimental setup is composed of our robotic needle insertion unit which allows for the insertion with the rotation and vibration, a polyvinyl chloride (PVC) phantom as an insertion target, a convex-shaped diaphragm model to mimic the breathing motion and USB camera (USB8MP02G-SFV, ELP, Japan) to measure the needle trajectory as show in Fig. 3. The breathing motion is achieved by moving the convex probe with a linear actuator (EAS4RX-D010-ARAA-1, Oriental motor, Japan) against the phantom in the direction perpen dicular to the needle insertion. The stiffness of the PVC phantom can be changed by altering the percentage of the plasticizer and softener (Super Liquid Plastic, M-F Manufacturing, USA). In this experiment, we measured the stiffness of a porcine lung by using an accurate universal tester (Autograph AG-IS 100 kN, Shimadzu, Japan) and decided the stiffness of the PVC phantom based on the measured stiffness of the porcine lung. Fig. 4 shows the measurement stiffness of the porcine lung and the PVC phantom with several ratios: 100% plasticizer, 0% softener by volume; 75% plasticizer, 25% softener by volume; 50% plasticizer, 50% softener by volume. Focusing on the rate of change of the stress σ with respect to the strain ε from 0 to 0.2, the stiffness of the PVC phantom with 75% ratio is similar to of the porcine lung. Then, we choose the 75% PVC phantom as the insertion target. To the phantom, we perform the needle insertion under three-way depths from the diaphragm model: 15, 30, and 45 mm during the breathing motion, and also under no breathing motion as

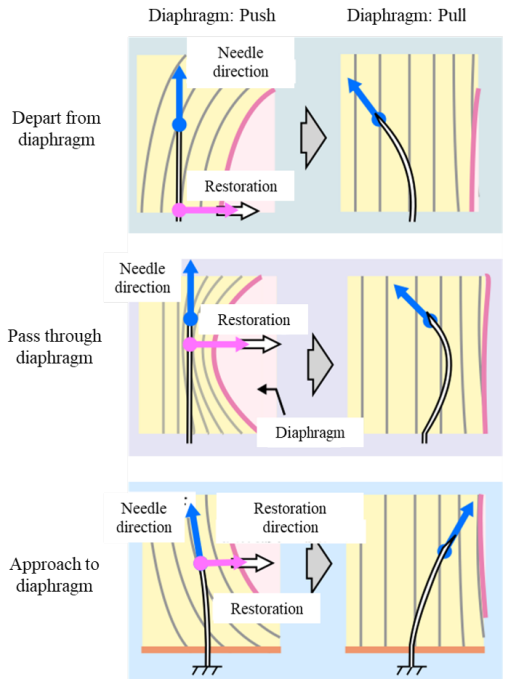

Fig. 6 Illustration of the assumption that the tissue deformation corresponding to the diaphragm motion causes the needle deflection.

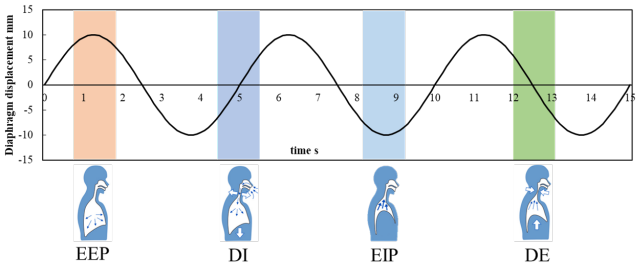

Fig. 7 Classification of breathing status: end expiratory pause (EEP), end inspiratory pause (EIP), during expiratory (DE), during inspiratory (DI).

the ground truth. The condition of the diaphragm is below: motion amplitude, 25 mm; frequency (δ_{breath}), 0.2 Hz (5 sec); waveform, sine curve, referring [43]. Also, to minimize the deflection due to the geometry of the fine needle, the bidirectional rotation is applied continuously during the insertion. Our robotic needle insertion system is mainly composed of a linear stage for the insertion motion and a stepper motor for the rotational motion [39]. The robotic needle insertion parameters are below: needle gauge, 25G (φ0.5 mm); needle length, 150 mm; insertion velocity (v_{ins}), 5 mm/s; insertion length, 120 mm; rotational speed (u_{rot}), 80 rpm. After finishing the needle insertion and stopping the breathing motion which corresponds to the released state of the phantom, the needle tip position is measured by the camera and the transverse distance between the needle tip and initial insertion path is calculated as the needle deflection. Insertion trials are eight to each insertion depth and Mann-Whitney *U* test with 95% confidence interval is used for the non-parametric statistical analysis.

Fig. 5 shows the result of the deflection in each insertion depth under breathing motion and without breathing motion. The result shows the deflection was increased depending on

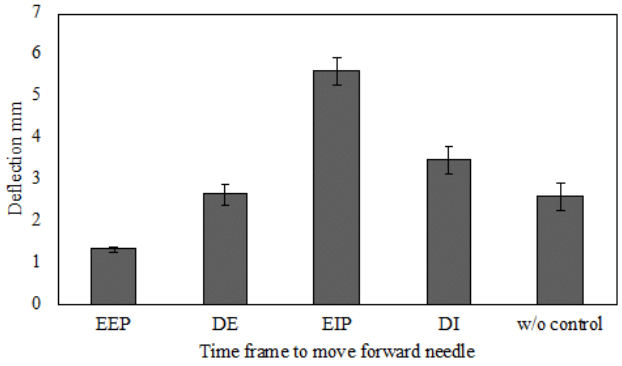

Fig. 8 The comparison of the deflection under applying the intermittent insertion with varying time frame to move forward the needle and the continuous insertion (w/o control).

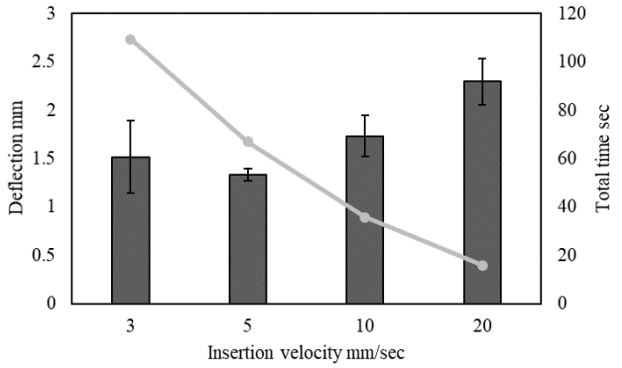

Fig. 9 The comparison of the deflection and total insertion time under applying the intermittent insertion in the EEP with varying insertion velocities.

the insertion depth. Please noted that the representative result is shown in the supplemental video. There was a significant difference between the depth of 15 mm and no breathing motion (p<0.05) and between the depth of 30 mm and no breathing motion (p<0.05), although there was no difference between the depth of 45 mm and no breathing motion. It suggests that the diaphragm motion causes an additional needle deflection given the needle trajectory is closed to the diaphragm. We assume that how deformed tissue where the needle will pass through affects the deflection. As shown in Fig. 6, given that the needle is passing through the deformed tissue due to the diaphragm motion, once releasing the pressure from the diaphragm, the needle may be strained toward the direction of the tissue restoration simultaneously. The degree of tissue restoration is remarkable near the diaphragm, which leads to further deflections. Thus, it is considerable that the deflection can be suppressed by moving forward the needle only during the time frame when the tissue is not compressed by the diaphragm.

C. Analysis of Timing to Conduct Intermittent Insertion

According to the previous experimental results, we assume that the state of breathing motion is one of the important facts to suppress the deflection. The state of breathing motion can be mainly categorized to four status: i) end expiratory pause (EEP), ii) end inspiratory pause (EIP), iii) during expiratory (DE), iv) during inspiratory (DI) as shown in Fig. 7. Then, we examine the intermittent needle insertion in each time frame and find an optimal insertion timing (t_{intm}) experimentally. In

this experiment, the insertion depth is fixed to 30 mm and the time range to move forward the needle in each time frame (δ_{ins}) is set at 1 sec. The EEP in this experiment corresponds to the released state of the phantom because the volume of lung is increased mostly and then the diaphragm model should not push the phantom. Conversely, the EIP corresponds to the compressed state of the phantom. The timing to conduct the intermittent insertion (t_{intm}) of the EEP, DE, EIP, DI is set at $\delta_{breath}/4$, $\delta_{breath}/2$, $\delta_{breath}3/4$, δ_{breath}, respectively. The other experimental conditions are the same as Section II-B.

Fig. 8 shows the result of the deflection by applying the intermittent needle insertion comparing each time frame. The deflection under moving forward the needle during EEP was minimized compared to other time frames, and significantly decreased than the deflection without applying the intermittent insertion (p<0.01). On the other hand, the deflection under during EIP was increased than the deflection without applying the intermittent insertion (p<0.01). Those results are following our assumption and indicates the EEP is the optimal state to conduct the intermittent insertion. Please noted that the representative result is shown in the supplemental video.

D. Analysis of Insertion Velocity

Although the insertion velocity was fixed at 5 mm/s in the above experiment, it may cause the procedure time and deflection. Given that the velocity is high, the procedure time can be decreased while the interaction force (e.g. puncture and friction forces) varies depending on the velocity [23], which leads to a further deflection possibly. Then, we need to further investigate the insertion velocity (v_{ins}) in terms of the balance between the procedure time and the needle deflection. In this experiment, four insertion velocities (3, 5, 10, and 20 mm/s) were performed. The timing to conduct the intermittent insertion was fixed at the EEP. The total insertion time was measured in addition to the deflection. The other experimental conditions are the same as Section II-C.

Fig. 9 shows the result of the deflection and total insertion time by applying the intermittent needle insertion in the EEP comparing each insertion velocity. Although there was no significant deference of the deflection between insertion velocities at 3 and 5 mm/s, the tendency of the deflection was slightly increased by increasing the velocities (between 5 and 10 mm/s, p<0.05; between 5 and 20 mm/s, p<0.01; between 10 and 20 mm/s, p<0.05). On the other hand, the total insertion time was decreased by increasing the insertion velocity. Those results are following our assumption and indicates the insertion velocity with 5 mm/s is experimentally optimal in terms of both deflection and total insertion time in this setup.

III. Evaluation

A. Experimental Setup

To verify the proposed intermittent insertion method in a realistic environment, we performed *ex vivo* experiments. As the insertion target, a porcine lung is used because of the similar property to human [44]. We control to put air into the porcine lung up to be a certain size (20x10x17 mm^3 in ref [45]) with an air compressor (ACP-13SLA EARTH MAN, Takagi, Japan) and a flow circuit including an electromagnetic proportional valve (PVQ31-6G-16-01, SMC, Japan), a flow sensor (PFM725S-01-C-MA-WS, SMC, Japan), a pressure sensor (PSE570-01, SMC, Japan) and a microprocessor (ESP-

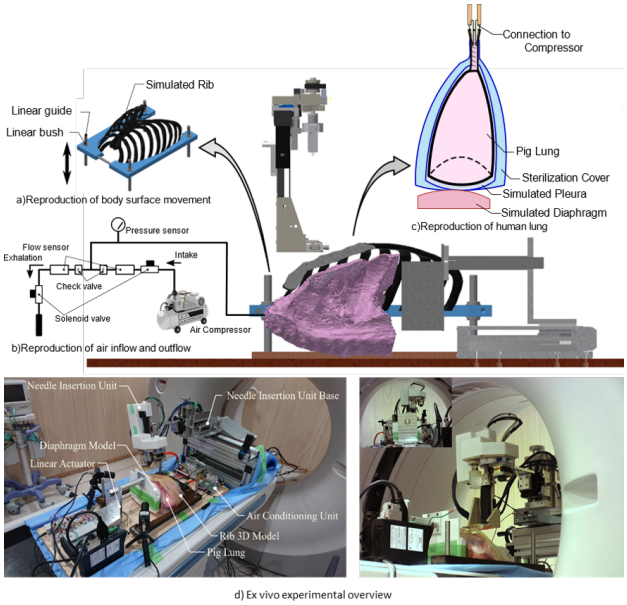

Fig. 10 The *ex vivo* experiment setup overview: (a) artificial rib allowing for the slide motion corresponding to the breathing motion; (b) air flow circuit; (c) conditions of porcine lung; (d) actual setup overview.

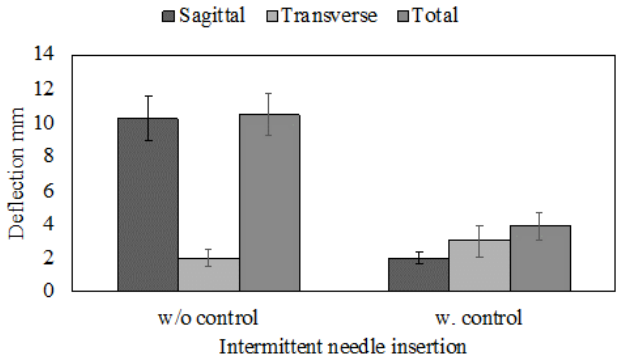

Fig. 11 The comparison of the deflection in the sagittal plane, transverse plane and 3D space between with and without the proposed intermittent insertion.

WROOM-32, Espressif Systems, China) as shown in Fig. 10. The porcine lung is covered with the sterilization bag and connected to the air compressor. Moreover, the porcine lung is put into a shell of artificial rib which can be slid in the front direction of body corresponding to the diaphragm motion. The diaphragm motion is achieved as same as Section II-B. The diaphragm model push to the bottom of the porcine lung. The air flow parameters are following: volume amplitude, 500 ml; frequency, 0.2 Hz, which is synchronized to the diaphragm motion. The parameter of the diaphragm motion is the same as Section II-B. The needle tip is tracked by using CT scan (Aquilion LB, Canon, Japan) because the needle trajectory is not visible in this *ex vivo* experiment. The CT slice interval is set at the minimum resolution of 0.5 mm. The deflections in transverse and sagittal planes are measured with the sequential CT slices after stopping the breathing motion. The three-dimensional (3D) deflection is calculated with the Pythagorean theorem using the measured deflections in both transverse and sagittal planes. The deflection measurement is performed with a DICOM viewer software (Array AOC, Array, Japan). The needle insertion is performed from twelve

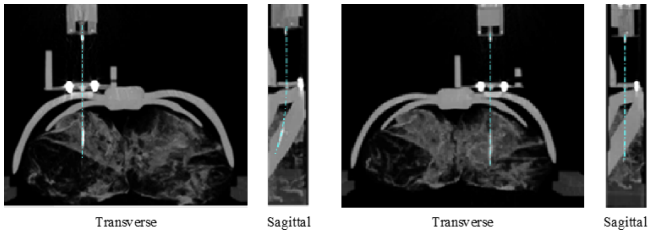

Fig. 12 The representative CT images under applying (a) the constant insertion and (b) the intermittent insertion. Blue dot lines show the actual needle path.

positions between ribs randomly in the direction perpendicularly to the CT bed. The deflection under applying the proposed intermittent insertion is compared to under applying the constant insertion (without the intermittent control). The insertion distance is set at 100 mm. The robotic needle insertion unit is attached to a base which allows the unit for the 3D positioning manually in the Cartesian coordinate. The insertion depth from the diaphragm model is set at 15 mm. Other experimental conditions are the same as Section II-B.

B. Result

Fig. 11 shows the result of the deflection comparing the proposed intermittent insertion with the constant insertion. Also, Fig. 12 shows the representative CT images in both cases. There is a significant difference of the 3D deflection between the intermittent and constant insertions (p<0.01). The deflection was decreased up to 3.87 ± 0.78 mm by applying the intermittent insertion. The deflection in the sagittal plans was significantly decreased by applying the intermittent insertion (p<0.01), although there is no difference of the deflection in the transverse plane between both insertions.

C. Discussion

The objective of this paper was to propose the intermittent insertion method with the fine needle which allows for reducing the needle deflection due to the breathing motion. In this paper, we developed the intermittent insertion method based on the PVC phantom study imitating the breathing motion and demonstrated the feasibility of the proposed insertion method through the *ex vivo* study with the porcine lung and the bench-top air flow circuit. The deflection could be successfully decreased without stopping the breathing motion by applying the proposed intermittent insertion. While, focusing on the deflection in the *ex vivo* results, the sagittal deflection can be decreased significantly by performing the intermittent insertion, although the difference of the transverse deflection between both insertions was not observed. We assume that the sagittal deflection is directly affected due to the diaphragm motion and then can be suppressed by the intermittent insertion. Meanwhile, the transverse deflection was still remaining even though the effect of the diaphragm motion for the transverse deflection may be low compared to for the sagittal deflection. It is considerable that the anatomical structure of the lung causes the deflection. In our previous paper [46], [47], we observed that the deflection was increased depending on the angle between the insertion direction and the tissue boundary, and the initial insertion angle into the surface of lung may cause the further deflection in this experiment. Then, in case of the lung needle insertion, the preoperative insertion path planning may be effective in addition to the intermittent insertion. Also, the internal anatomical structure of the porcine lung may cause the further deflection, which is the significant difference of the experimental setup between the PVC phantom and *ex vivo* studies. The lung includes a number of lung alveolus and alveolar duct. Given that the interaction force occurs during the needle passing through the internal structures, the deflection may be increased compared to the PVC phantom. We experimentally acquired and compared insertion force data with a force sensor (Nano 17 force/torque sensor, ATI Industrial Automation, USA) attached to the robotic needle insertion unit during the needle insertion into the porcine lung with and without air (see Appendix). The acquired force data showed that the peak force was observed during puncturing the alveolar duct, although there were few differences of the sequential forces between with and without air into the lung. Then, in addition to the insertion angle, taking account the position of the alveolar duct into the path planning algorism may be effective.

The limitation of this paper is described below. This paper served the concept of intermittent insertion method and presented experimental results. Meanwhile, we didn't address the quantitative control design and the needle deflection model. Subsequently, the insertion parameters including the insertion and rotation velocities and the time duration for the intermittent insertion were not optimized, although several patterns of the insertion parameter were examined through the PVC phantom study. Especially, the time frame in the intermittent insertion (δ_{ins}) was fixed at 1 sec, which may cause the effect for the deflection and total procedure time. As same as the insertion velocity, the procedure time can be decreased given that the time frame is increased, since the distance the needle can move in each breath cycle is increased. Meanwhile, the excessive wide range will stretch into next breath motion status (e.g. the excessive wide range at EEP will penetrate the DE and DI), which may cause the deflection. Additionally, the needle insertion force/torque during the breathing motion was not analyzed in those experiments. Given that changes of the interaction force between the needle and tissue over time corresponds to the breathing status, it enables to develop the closed-loop control system without the imaging feedback. We also assume that it enables to compensate the needle trajectory by integrating the concept of the intermittent insertion control into the needle steering. To achieve that, the needle-tissue interaction force model and the needle tip tracking method are required for estimating the needle trajectory. Meanwhile, there are few researches focusing on the analyses of the needle-tissue interaction and the deflection in the lung needle insertion. Then, it is necessary to further investigate the needle-tissue interaction during the breathing motion. While, the needle tip tracking in the lung needle insertion is challenging because it is difficult to acquire the real-time image-based feedback. As an alternative approach, we may use sensor-based approaches including fiber bragg grading (FBG) and electromagnetic (EM) sensors, which also have the technical challenging to embed sensors into the fine needle.

Regarding the experimental setup, the synchronization of the needle insertion and the breathing motion was performed in an ideal situation that the needle insertion could be controlled under tracking the diaphragm motion real-time through the serial communication. In clinical situations, the

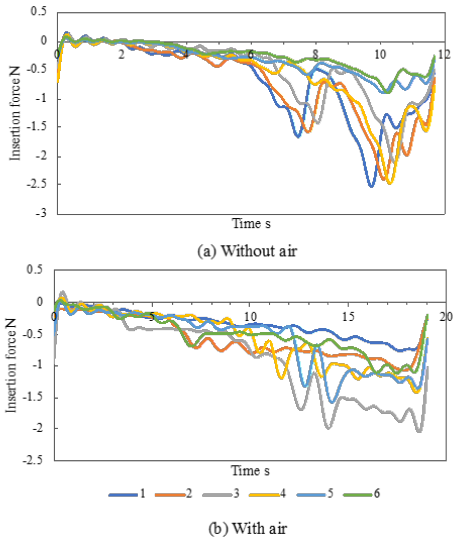

Fig. A1 The comparison of insertion force into the porcine lung with and without air.

diaphragm motion cannot be tracked by using this setup. Then, it is necessary to integrate a feedback system which can monitor the breathing status into our proposed system as shown in Fig. 2. There are related works to estimate the status of breathing motion by tracking the motion of body surface [37], [48].

IV. Conclusion

This paper describes the intermittent insertion control method to decrease the needle deflection adapting the lung deformation due to the breathing motion. The novelty of this method is to allow for the accurate needle insertion without stopping the breath, which will contribute to decrease the discomfort and the amount of radiation exposure for patients. The intermittent insertion is to move forward the fine needle during a certain time frame (end expiratory pause) that the needle deflection barely occurs since the lung is not deformed by the diaphragm motion. The feasibility of the proof-of-concept was validated through the PVC phantom and *ex vivo* experiments. The results showed that the deflection can be suppressed up to 1.3 mm and 3.9 mm in the PVC phantom and *ex vivo* experiments, respectively, and indicates that it is ready to further studies on animals.

Appendix

We experimentally acquired and compared insertion force data with the porcine lung with and without air. The breathing motion was stopped totally. Six trials were performed in each condition. Fig. A1 shows the series of insertion force data.

Acknowledgment

We gratefully acknowledge Mr. R. Matsumoto and our cancer research team at the Iwata laboratory, Waseda University for their technical assistance, and Rt. M. Oshida and staffs at BSL-48 International Clinic for providing experimental environment.

References

[1] C. De Margerie-Mellon, C. De Bazelaire, and E. De Kerviler, "Image-guided biopsy in primary lung cancer: Why, when and how," *Diagn. Interv. Imaging*, vol. 97, no. 10, pp. 965–972, 2016.

[2] J. C. Zhu, T. D. Yan, and D. L. Morris, "A systematic review of radiofrequency ablation for lung tumors," *Ann. Surg. Oncol.*, vol. 15, no. 6, pp. 1765–1774, 2008.

[3] M. M. Arnolli, M. Buijze, M. Franken, K. P. de Jong, D. M. Brouwer, and I. A. M. J. Broeders, "System for CT-guided needle placement in the thorax and abdomen: A design for clinical acceptability, applicability and usability," *Int. J. Med. Robot. Comput. Assist. Surg.*, vol. 14, no. 1, p. e1877, 2018.

[4] R. Kloeckner, D. P. Dos Santos, J. Schneider, L. Kara, C. Dueber, and M. B. Pitton, "Radiation exposure in CT-guided interventions," *Eur. J. Radiol.*, vol. 82, no. 12, pp. 2253–2257, 2013.

[5] O. Efesoylu, M. Bozlu, S. Cayan, and E. Akbay, "Complications of transrectal ultrasound-guided 12-core prostate biopsy: a single center experience with 2049 patients," *Türk Üroloji Dergisi/Turkish J. Urol.*, vol. 39, no. 1, pp. 6–11, 2013.

[6] N. Tomiyama *et al.*, "CT-guided needle biopsy of lung lesions: A survey of severe complication based on 9783 biopsies in Japan," *Eur. J. Radiol.*, vol. 59, no. 1, pp. 60–64, 2006.

[7] A. Oikonomou, F. R. Matzinger, J. M. Seely, C. J. Dennie, and P. J. Macleod, "Ultrathin needle (25 G) aspiration lung biopsy: Diagnostic accuracy and complication rates," *Eur. Radiol.*, vol. 14, no. 3, pp. 375–382, 2004.

[8] N. Abolhassani, R. Patel, and M. Moallem, "Needle insertion into soft tissue: A survey," *Med. Eng. Phys.*, vol. 29, pp. 413–431, 2007.

[9] E. Dehghan, O. Goksel, and S. E. Salcudean, "A comparison of needle bending models.," *Med. Image Comput. Comput. Assist. Interv.*, vol. 9, no. Pt 1, pp. 305–312, 2006.

[10] C. Rossa, M. Khadem, R. Sloboda, N. Usmani, and M. Tavakoli, "Adaptive Quasi-Static Modelling of Needle Deflection during Steering in Soft Tissue," *IEEE Robot. Autom. Lett.*, vol. 1, no. 2, pp. 916–923, 2016.

[11] S. Misra, K. B. Reed, B. W. Schafer, K. T. Ramesh, and a. M. Okamura, "Mechanics of Flexible Needles Robotically Steered through Soft Tissue," *Int. J. Rob. Res.*, vol. 29, no. 13, pp. 1640–1660, 2010.

[12] R. J. Webster III, N. J. Cowan, G. S. Chirikjian, and a M. Okamura, "Nonholonomic Modelling of Needle Steering," *Int. J. Rob. Res.*, vol. 25, no. 5–6, pp. 509–525, 2006.

[13] G. Li *et al.*, "A novel analytical approach to the prediction of respiratory diaphragm motion based on external torso volume change," *Phys. Med. Biol.*, vol. 54, no. 13, pp. 4113–4130, 2009.

[14] M. Mccormack, A. Duclos, M. Latour, and M. Hélène, "Effect of needle size on cancer detection , pain , bleeding and infection in TRUS-guided prostate biopsies : a prospective trial," *Can. Urol. Assoc. J.*, vol. 6, no. 2, pp. 97–101, 2012.

[15] H. S. Gill and M. R. Prausnitz, "Does needle size matter?," *J. Diabetes Sci. Technol.*, vol. 1, no. 5, pp. 725–729, 2007.

[16] H. Egekvist, P. Bjerring, and L. Arendt-Nielsen, "Pain and mechanical injury of human skin following needle insertions," *Eur. J. Pain*, vol. 3, no. 1, pp. 41–49, 1999.

[17] C. Manno *et al.*, "Predictors of bleeding complications in percutaneous ultrasound-guided renal biopsy," *Kidney Int.*, vol. 66, no. 4, pp. 1570–1577, 2004.

[18] "Consensus of Percutaneous Lung Needle Biopsy Statement from Japanese Society of Lung Needle Biopsy," pp. 256–261, 2007.

[19] K. Izumi, R. Tsumura, and H. Iwata, "Quantitative Evaluation of Bleeding during Blood Vessel Puncture Caused by Fine Needle in Lower Abdomen," *2019 41st Annu. Int. Conf. IEEE Eng. Med. Biol. Soc.*, pp. 5862–5866, 2019.

[20] D. Gao, Y. Lei, and H. Zheng, "Needle steering for robot-assisted insertion into soft tissue: A survey," *Chinese J. Mech. Eng.*, vol. 25, no. 4, pp. 629–638, 2012.

[21] C. Rossa and M. Tavakoli, "Issues in closed-loop needle steering," *Control Eng. Pract.*, vol. 62, pp. 55–69, 2017.

[22] B. K. B. Reed *et al.*, "Robot-Assisted Needle Steering," *IEEE Robot. Aoutomation Mag.*, no. December, pp. 35–46, 2011.

[23] D. J. van Gerwen, J. Dankelman, and J. J. van den Dobbelsteen, "Needle–tissue interaction forces – A survey of experimental data," *Med. Eng. Phys.*, vol. 34, no. 6, pp. 665–680, 2012.

[24] C. Yang, Y. Xie, S. Liu, and D. Sun, "Force Modeling, Identification, and Feedback Control of Robot-Assisted Needle Insertion : A Survey of the Literature," *Sensors*, vol. 18, no. 2, pp. 561-1–38, 2018.
[25] M. Abayazid, R. J. Roesthuis, R. Reilink, and S. Misra, "Integrating deflection models and image feedback for real-time flexible needle steering," *IEEE Trans. Robot.*, vol. 29, no. 2, pp. 542–553, 2013.
[26] J. Carriere, M. Khadem, C. Rossa, N. Usmani, and R. Sloboda, "Surgeon-in-the-Loop 3-D Needle Steering Through Ultrasound-Guided Feedback Control," *IEEE Robot. Autom. Lett.*, vol. 3, no. 1, pp. 469–476, 2018.
[27] T. K. Adebar, A. E. Fletcher, and A. M. Okamura, "3-D ultrasound-guided robotic needle steering in biological tissue," *IEEE Trans. Biomed. Eng.*, vol. 61, no. 12, pp. 2899–2910, 2014.
[28] G. J. Vrooijink, M. Abayazid, S. Patil, R. Alterovitz, and S. Misra, "Needle path planning and steering in a three-dimensional non-static environment using two-dimensional ultrasound images," *Int. J. Rob. Res.*, vol. 33, no. 10, pp. 1361–1374, 2014.
[29] P. Mignon, P. Poignet, and J. Troccaz, "Automatic Robotic Steering of Flexible Needles from 3D Ultrasound Images in Phantoms and Ex Vivo Biological Tissue," *Ann. Biomed. Eng.*, vol. 46, no. 9, pp. 1385–1396, 2018.
[30] R. Seifabadi, E. E. Gomez, F. Aalamifar, G. Fichtinger, and I. Iordachita, "Real-time tracking of a bevel-tip needle with varying insertion depth: Toward teleoperated MRI-guided needle steering," *IEEE Int. Conf. Intell. Robot. Syst.*, pp. 469–476, 2013.
[31] N. A. Patel *et al.*, "Closed-loop asymmetric-tip needle steering under continuous intraoperative MRI guidance," *Proc. Annu. Int. Conf. IEEE Eng. Med. Biol. Soc. EMBS*, vol. 2015-Novem, pp. 4869–4874, 2015.
[32] D. Glozman and M. Shoham, "Image-guided robotic flexible needle steering," *IEEE Trans. Robot.*, vol. 23, no. 3, pp. 459–467, 2007.
[33] N. Shahriari, W. Heerink, T. van Katwijk, E. Hekman, M. Oudkerk, and S. Misra, "Computed tomography (CT)-compatible remote center of motion needle steering robot: Fusing CT images and electromagnetic sensor data," *Med. Eng. Phys.*, vol. 45, pp. 71–77, 2017.
[34] N. Shahriari, E. Hekman, M. Oudkerk, and S. Misra, "Design and evaluation of a computed tomography (CT)-compatible needle insertion device using an electromagnetic tracking system and CT images," *Int. J. Comput. Assist. Radiol. Surg.*, vol. 10, no. 11, pp. 1845–1852, 2015.
[35] T. Hiraki *et al.*, "Robotic needle insertion during computed tomography fluoroscopy–guided biopsy: prospective first-in-human feasibility trial," *Eur. Radiol.*, vol. 30, no. 2, pp. 927–933, 2020.
[36] S. Jiang, W. Yuan, Y. Yang, D. Zhang, N. Liu, and W. Wang, "Modelling and analysis of a novel CT-guided puncture robot for lung brachytherapy," *Adv. Robot.*, vol. 31, no. 11, pp. 557–569, 2017.
[37] Y. Zhou, K. Thiruvalluvan, L. Krzeminski, W. H. Moore, Z. Xu, and Z. Liang, "An experimental system for robotic needle biopsy of lung nodules with respiratory motion," *2011 IEEE Int. Conf. Mechatronics Autom. ICMA 2011*, pp. 823–830, 2011.
[38] S. Badaan *et al.*, "Does needle rotation improve lesion targeting?," *Int. J. Med. Robot. Comput. Assist. Surg.*, vol. 7, pp. 138–147, 2011.
[39] A. Majewicz, J. J. Siegel, A. a Stanley, and A. M. Okamura, "Design and Evaluation of Duty-Cycling Steering Algorithms for Robotically-Driven Steerable Needles," *Proc. IEEE Int. Conf. Robot. Autom.*, pp. 5883–5888, 2014.
[40] D. S. Minhas, J. a. Engh, M. M. Fenske, and C. N. Riviere, "Modeling of needle steering via duty-cycled spinning," *Annu. Int. Conf. IEEE Eng. Med. Biol. - Proc.*, pp. 2756–2759, 2007.
[41] R. Tsumura, Y. Takishita, Y. Fukushima, and H. Iwata, "Histological Evaluation of Tissue Damage Caused by Rotational Needle Insertion," *Proc. Annu. Int. Conf. IEEE Eng. Med. Biol. Soc.*, pp. 5120–5123, 2016.
[42] R. Tsumura, Y. Takishita, and H. Iwata, "Needle Insertion Control Method for Minimizing Both Deflection and Tissue Damage," *J. Med. Robot. Res.*, vol. 3, no. 4, pp. 1842005-1–9, 2018.
[43] P. Vostatek, D. Novák, T. Rychnovský, and Š. Rychnovská, "Diaphragm Postural Function Analysis Using Magnetic Resonance Imaging," *PLoS One*, vol. 8, no. 3, 2013.
[44] J. E. Nichols *et al.*, "Production and transplantation of bioengineered lung into a large-animal model," *Sci. Transl. Med.*, vol. 10, no. 452, 2018.
[45] G. H. Kramer, K. Capello, B. Bearrs, A. Lauzon, and L. Normandeau, "Linear dimensions and volumes of human lungs obtained from CT images," *Health Phys.*, vol. 102, no. 4, pp. 378–383, 2012.
[46] R. Tsumura, J. S. Kim, H. Iwata, and I. Iordachita, "Preoperative Needle Insertion Path Planning for Minimizing Deflection in Multilayered Tissues," *IEEE Robot. Autom. Lett.*, vol. 3, no. 3, pp. 2129–2136, 2018.
[47] R. Tsumura and H. Iwata, "Trajectory Planning for Abdominal Fine Needle Insertion Based on Insertion Angles," *IEEE Robot. Autom. Lett.*, vol. 2, no. 2, pp. 1226–1231, 2017.
[48] S. F. Atashzar, I. Khalaji, M. Shahbazi, A. Talasaz, R. V. Patel, and M. D. Naish, "Robot-assisted lung motion compensation during needle insertion," *Proc. - IEEE Int. Conf. Robot. Autom.*, pp. 1682–1687, 2013.